Hindawi Publishing Corporation
Journal of Nanomaterials
Volume 2015, Article ID 894353, 6 pages
http://dx.doi.org/10.1155/2015/894353

Research Article

Improvement in Tracing Quantum Dot-Conjugated Nanospheres for *In Vivo* Imaging by Eliminating Food Autofluorescence

Chul-Kyu Park[1] and Hoonsung Cho[2]

[1]*Department of Physiology, College of Medicine, Gachon University, Incheon 406-799, Republic of Korea*
[2]*School of Materials Science & Engineering, Chonnam National University, Gwangju 500-757, Republic of Korea*

Correspondence should be addressed to Hoonsung Cho; cho.hoonsung@jnu.ac.kr

Received 12 June 2015; Accepted 18 August 2015

Academic Editor: Aran Son

Fluorescence imaging using fluorescent probes has demonstrated long-term stability and brightness suitable for *in vivo* deep-tissue imaging, but it also allows intense background fluorescence associated with food in the near-infrared (IR) range. We investigated effects of changing rodent diet on food autofluorescence, in the presence of quantum dots-conjugated magnetic nanospheres (QD-MNSs). Replacement of a regular rodent diet with a purified diet has great improvement in removing autofluorescence in the near-infrared range ideal for *in vivo* fluorescence imaging. By feeding a purified diet for eliminating ingredients impairing desirable fluorescence signals in the near-IR range, food autofluorescence was clearly eliminated and fluorescence probes, QD-MNSs, introduced by i.v. injection were effectively traced in a mouse by a distinctive signal-to-noise ratio.

1. Introduction

Imaging technologies of tracking fluorescent probes, such as fluorophores, quantum dots, phosphors, and other fluorescent reporters, are rapidly expanding for early diagnosis of disease [1, 2], noninvasive and quantitative screening [3, 4], and therapeutic treatment [5–7]. Of these, applications of quantum dots (QDs) have great potential of *in vivo* fluorescence imaging, in particular, in small animal studies [8–10], due to the ability to exhibit intense emissions in the near-infrared range, which is ideal for deep-tissue investigations [11]. Although fluorescence imaging by QDs has demonstrated long-term stability and brightness suitable for *in vivo* deep-tissue imaging, it also allows intense background fluorescence associated with food in the near-infrared range. Generating background fluorescence, called autofluorescence, occurs in the abdomen of mice and impairs to select fluorescence of interest in any small animal imaging studies. It is due largely to the chlorophyll component, called alfalfa, of many plant-based ingredients used in regular mouse diet. Regular rodent diets generally contain large amounts of alfalfa (chlorophyll). Because intestinal autofluorescence interferes with the signal from fluorescent probes localized in or near the abdomen and also mimics the excretion and/or accumulation of probes in the intestine, it is difficult to confirm fluorescence of interest without separation of internal organs by incision of mice [12].

There have been several publications where replacing a regular rodent diet with alfalfa-free rodent diet can minimize or eliminate food autofluorescence [13–16]. However, it is still unclear how changing rodent diets has an effect on autofluorescence, particularly when taking into account the presence of intense fluorescent probes. In this report, therefore, since a purified diet that does not contain chlorophyll has reduced autofluorescence in the near-IR range [13], the purified diet (D10001a, Research Diets, Inc.) is fed to mice instead of a regular rodent diet and then its effect on autofluorescence is measured in the presence of the fluorescent probes, quantum dot-conjugated magnetic nanospheres (QD-MNSs). Tracing QD-MNSs administrated via intravenous injection in the purified diet-fed mouse is evaluated for future use of the purified rodent diet for *in vivo* fluorescence imaging.

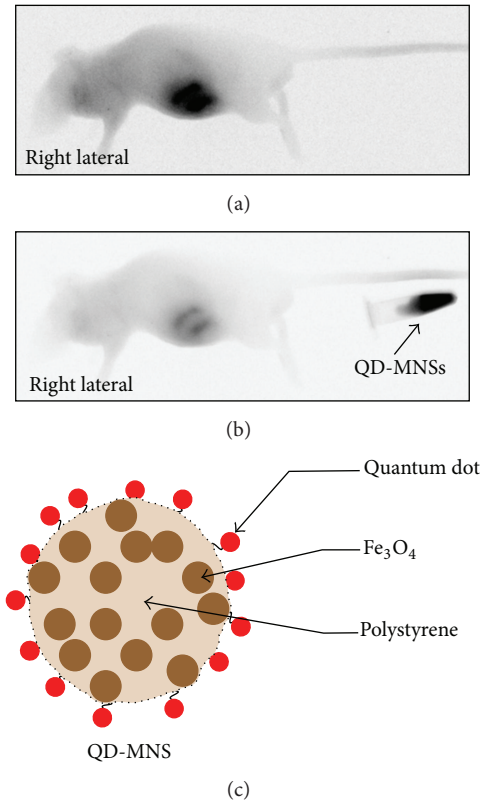

Figure 1: *In vivo* fluorescence images of which regular diets were fed. Dark areas indicate fluorescent signals; (a) in the absence of fluorescent materials; (b) in the presence of fluorescence marker (Qdots-conjugated MNSs); (c) conjugation of amine-functionalized quantum dots (QDs) to the surface of MNS. There are intense autofluorescence signals in the abdominal region of the mouse, even regardless of strong fluorescence sources. These images are taken in the identical conditions (excitation filter: 720 nm, emission filter: 790 nm, and exposure time: 10 sec).

2. Materials and Method

Fluorescence probes used in this study were synthesized by conjugation of QDs on the surface of magnetic nanospheres (MNS) desired for localized cancer diagnosis. Qdot 800 ITK amino (PEG) quantum dots with emission wavelength of 800 nm (Invitrogen Corporation, Carlsbad, CA) were immobilized on the MNSs by a combined strategy of covalent coupling and electrostatic adsorption [12]. Carboxylate-functionalized MNSs were washed three times with phosphate-buffered saline, pH 7.4 (PBS), and incubated for 20 min at room temperature in 1-(3-dimethylaminopropyl)-3-ethylcarbodiimide hydrochloride (EDC) solution (400 mM) and N-hydroxysuccinimide (NHS) solution (100 mM). The NHS-activated MNSs were conjugated to amino-functionalized QDs. The regular rodent diet commonly used in laboratory research is Techlad Global Rodent Diet (LM-485, Harlan Tecklad, WI) and the purified diet (D10001i, Research Diets, NJ) was purchased for reducing autofluorescence. All *in vivo* fluorescent images are taken using the Kodak Imaging station (Carestream Health, Inc., Rochester, NY), in most cases, with 720 nm excitation and 790 nm emission. Fluorescence images were monitored before and after intravenous injection of QD-MNS (10 mg/mL in PBS, 100 μL of QD-MNS per animal) in nude mice via tail vein. Three animals were used in each condition and one image was chosen for the figure because there were no substantial differences among the animals. This study was approved by the Institutional Animal Use and Care Committee (IACUC) at the University of Cincinnati in compliance with relevant State and Federal Regulations.

3. Results and Discussion

Figure 1 shows the typical monochromatic *in vivo* fluorescence images of the mouse which is fed the regular diet, taken with 693 nm laser as an excitation source and 720 nm excitation and 790 nm emission set. As usual, intense autofluorescent signals were observed in the abdominal region, indicating that autofluorescence in this emission range is mostly based on the rodent diet (Figure 1(a)). For the effect of fluorescent probes on the autofluorescence, QD-MNSs emitting 800 nm wavelength were introduced as a fluorescent marker for evaluating changes to the fluorescent image of mouse when the fluorescent marker is applied to the mouse. In the presence of the fluorescent marker (Figure 1(b)), the signal in the abdominal region is much dimmer than that without the fluorescent marker, yet there is still strong autofluorescence visible. This intense autofluorescence has to be removed for further *in vivo* fluorescent research.

The optical image in Figure 2 shows the regular rodent diet (Techlad Global Rodent Diet, LM-485, Harlan Tecklad,

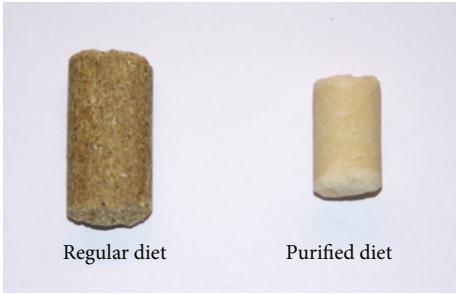

Figure 2: Optical image of two rodent diets for this research: regular diet and purified diet.

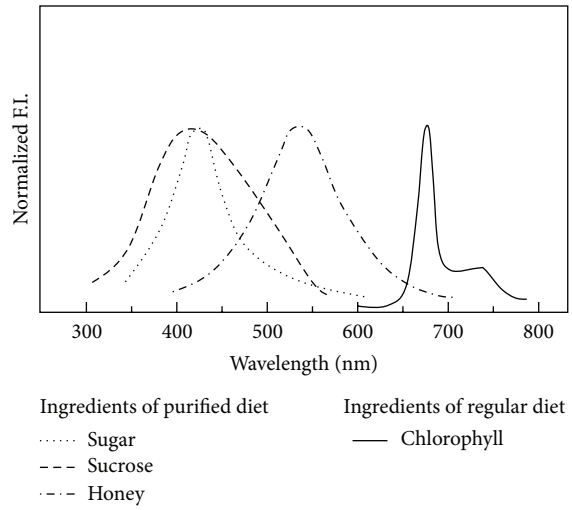

Figure 3: Fluorescence spectra recorded from pure honey, sucrose, cane sugar syrup, and chlorophyll. Reproduced from [17–19].

WI) and the purified diet (D10001i, Research Diets, NJ) purchased for reducing autofluorescence. The main ingredients of the Techlad Global Rodent Diet, LM-485, are ground corn, soybean meal, alfalfa meal, and wheat middlings. It is reported that, among the ingredients, alfalfa meal containing chlorophyll, one of vital components for photosynthesis, is responsible for the autofluorescence [20]. In particular, when the chromophore pigments, chlorophyll, are involved in photosynthesis reactions, called photosystems I and II, a small portion of the excess energy is not absorbed at higher energy state and emanates chlorophyll fluorescence [21]. At physiological temperature, the chlorophyll fluorescence spectrum exhibits the highest peak at 682 nm and a broad shoulder peak around 740 nm and extends into near-infrared (IR) range (800 nm) [17]. This chlorophyll fluorescence contributes to increasing autofluorescence in a range of near-IR in an abdominal region of a mouse and obscure optical tracing of fluorescent probes. However, the purified diet (D10001i) is mostly made of sucrose, casein, and corn starch. It also emanates intense fluorescent signals; however, it ranges over much shorter emission wavelength (around 400~650 nm) than that of the regular diet [18, 19, 22]. The fluorescence of the purified diet is mainly introduced by one of the main ingredients, sucrose. Sucrose, a crystalline disaccharide carbohydrate ($C_{12}H_{22}O_{11}$), is primarily made of glucose and fructose and exhibits the maximum intensity of fluorescence peak at 420 nm and spreads out the fluorescence spectrum from 350 nm to 550 nm [18]. It is also reported that honey, having same major ingredients with sucrose (glucose and fructose), emanates intense fluorescence in the range between 400 nm and 650 nm and exhibits the maximum fluorescence peak at 550 nm with 460 nm excitation (Figure 3) [19]. These specific fluorescence properties of the two rodent diets have been demonstrated in Figure 4, showing the fluorescent images under the various filter sets: (a) 465 nm excitation and 535 nm emission, (b) 535 nm excitation and 600 nm emission, (c) 625 nm excitation and 700 nm emission, and (d) 720 nm excitation and 790 nm emission. As described before, at the wavelength of 700 nm emission (Figure 4(c)), the fluorescence signal of the regular diet is the strongest due to the chlorophyll fluorescence. When imaged at the other wavelengths, such as 535 nm, 600 nm, and 790 nm, the regular diet exhibits weaker fluorescence than that at 700 nm, but still considerable amount of signals enough to impair distinctive fluorescence tracing images. However, the fluorescence of the purified diet shows the intense signals at the 535 nm emission wavelength (Figure 4(a)) and much weaker fluorescence at 600 nm (Figure 4(b)). In the near-infrared range around 650–900 nm, which is actually an applicable region for *in vivo* fluorescence imaging due to the low body autofluorescence, the purified diet has no significant fluorescence (Figures 4(c) and 4(d)), and it is thus expected to have great advantage of reducing autofluorescence by feeding them to a mouse.

Figure 5 shows how the purified diet affects *in vivo* fluorescence imaging of mice. The mouse food was switched from the regular diet to the purified diet and the whole body of the mouse was imaged daily. In Figures 5(a) and 5(b), as black arrows indicate intense autofluorescence induced by the rodent diet in the abdominal region, there are still strong fluorescent signals in the intestinal track at the early period of 1 day after being fed the purified diet. In the time course study, a switch in diet requires at least 3 days to clear residual autofluorescence in the abdominal region. On the third day after replacement of the rodent diet, the food autofluorescence has clearly disappeared (Figure 5(c)) and it kept being sustained as long as the mouse is fed the purified diet (Figure 5(d)). Even though the major autofluorescence in the abdominal region by the food has been eliminated, there is still but weak autofluorescence present over the mouse body with even contrast, which is skin autofluorescence emanating from the whole body (Figures 5(c) and 5(d)). However, it has been clearly shown that the skin autofluorescence is not a consideration any more in Figure 6.

Figure 6 shows *in vivo* fluorescence imaging of a mouse being fed the purified diet for two weeks before and after the administration of QD-MNSs into the tail vein of a mouse. While strong intensity of autofluorescence was observed in abdominal region of a mouse fed the regular rodent diet even in the presence of QD-MNS probes (Figure 1(b)), an autofluorescence signal of a mouse switched to the purified diet significantly reduced food autofluorescence

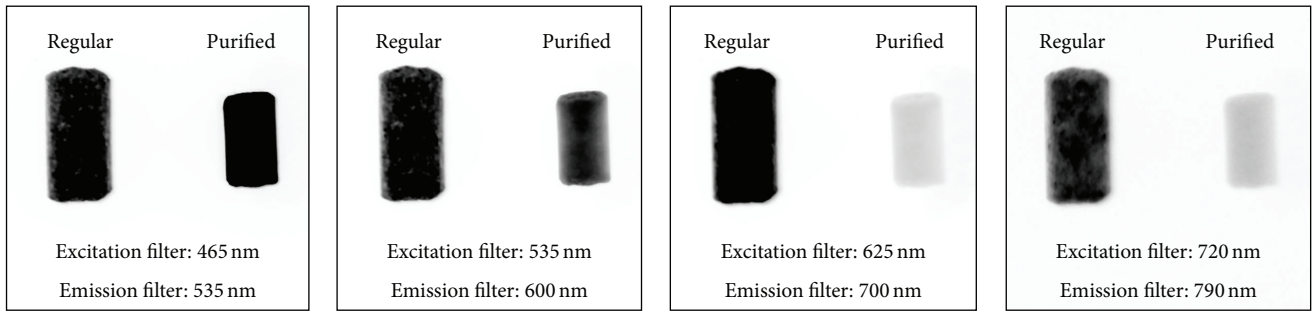

Figure 4: Fluorescent intensities of purified diet in comparison to regular diet under various filter sets. Strong fluorescence of regular diet was observed through the whole range of wavelength. It is clear that fluorescent signal of regular diet is lower than that of purified diet in 535 nm wavelength (a), and *vice versa* in near-infrared region ((c) and (d)). In contrast to regular diet, fluorescence of purified diet is decreased as the range of the emission wavelength is increased.

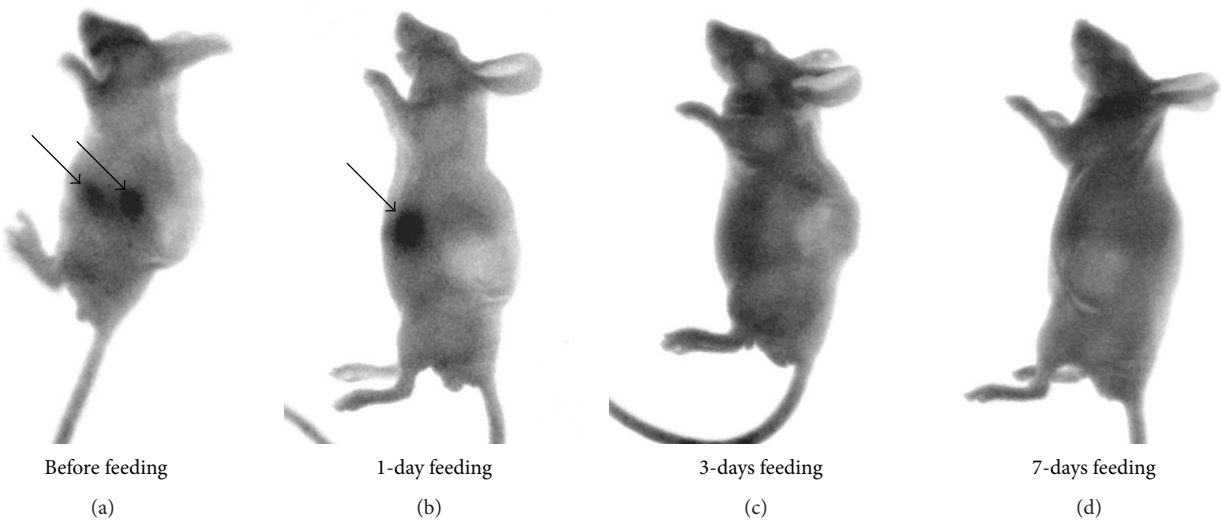

Figure 5: A mouse switched from regular mouse food to a purified diet (D10001a) was imaged daily to record the reduction of autofluorescence from the abdominal region. Black signals represent the autofluorescence in the range of 800 nm in wavelength. After 3 days' feeding, intense autofluorescence in the abdominal region has disappeared and light autofluorescence was shown uniformly over the whole body (excitation filter: 720 nm, emission filter: 790 nm).

in the abdominal region (Figure 6(a)). It is clear that the purified diet made great improvement in signal-to-noise ratio, in particular when a fluorescence image was taken with QD-MNSs probes (the right image of Figure 6(a)). In the presence of QD-MNSs probes, autofluorescence of the mouse is barely visible and much less likely to interfere with desirable fluorescence signals, while QD-MNSs probes achieve marked contrast to the autofluorescence. Removal of body autofluorescence would enable effectively increasing the sensitivity of the optical detection system and even detecting weak fluorescent signals. The QD-MNSs probes were then introduced to the mouse by i.v. tail injection. Thirty minutes after injection, significant fluorescence associated with QD-MNSs was clearly discernable in the abdominal region (Figure 6(b)). By comparing with the autofluorescence images in Figure 5, the images taken after i.v. injection show that the fluorescent probes are located in the upper area compared to those of autofluorescence, probably indicating that the probes are accumulated in a liver or a spleen. It is now clearly shown that the fluorescent signals obtained after administration of fluorescent probes indicate exactly where the probes are accumulated and located in the body and can be verified as a desirable signal without sacrificing the mouse.

4. Conclusions

In conclusion, based on fluorescence comparisons of a regular diet and a purified diet themselves under various regions of wavelength, it is obtained that feeding a purified diet is the most effective method in removing autofluorescence in 700–800 nm range, which is known for an ideal region of *in vivo* fluorescence imaging. By replacement of a regular rodent diet with a purified diet intended for eliminating ingredients

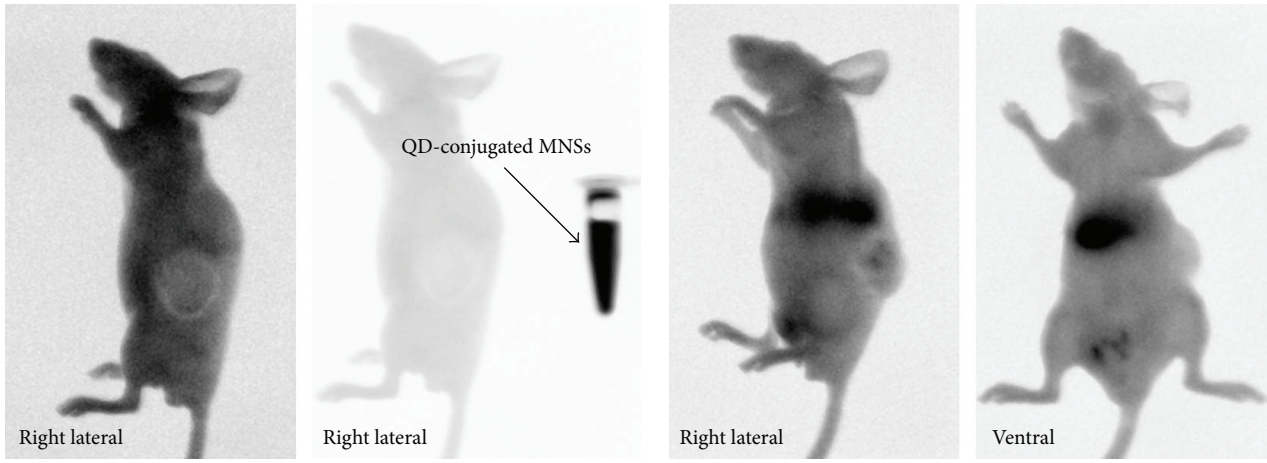

(a) Before i.v. injection (b) 30 min after i.v. injection

Figure 6: *In vivo* images before and after intravenous injection of QD-MNS in a nude mouse being fed the purified diet (D10001a). There is no autofluorescence in the mouse fed the purified diet with the presence of fluorescent marker (a). It is clear that the black intense fluorescence signals indicate QD-MNS accumulation in the abdominal region 30 min after injection (b) (excitation filter: 720 nm, emission filter: 790 nm).

impairing desirable fluorescence signals in the near-IR range, autofluorescence by food was clearly removed and fluorescence probes, QD-MNSs, introduced by i.v. injection were effectively traced in a mouse by a distinctive signal-to-noise ratio. The QD-MNS exhibited strong fluorescent emission in the near-IR range. The fluorescence images obtained from mice fed the purified rodent diet facilitate evaluation of fluorescent probes as an innovative, multifunctional nanodevice for biomedical applications and support further research of *in vivo* fluorescence imaging.

Conflict of Interests

The authors declare no conflict of interests.

Acknowledgments

This work was supported by the Gachon University research fund of 2014 (GCU-2014-5095) and by a grant of the Korean Health Technology R&D Project, Ministry of Health & Welfare, Republic of Korea (HI14C1842).

References

[1] R. Eichhorn, G. Wessler, M. Scholz et al., "Early diagnosis of melanotic melanoma based on laser-induced melanin fluorescence," *Journal of Biomedical Optics*, vol. 14, no. 3, Article ID 034033, 2009.

[2] W.-F. T. Lai, C.-H. Chang, Y. Tang, R. Bronson, and C.-H. Tung, "Early diagnosis of osteoarthritis using cathepsin B sensitive near-infrared fluorescent probes," *Osteoarthritis and Cartilage*, vol. 12, no. 3, pp. 239–244, 2004.

[3] F. Gu, L. Zhang, B. A. Teply et al., "Precise engineering of targeted nanoparticles by using self-assembled biointegrated block copolymers," *Proceedings of the National Academy of Sciences of the United States of America*, vol. 105, no. 7, pp. 2586–2591, 2008.

[4] S. Keren, C. Zavaleta, Z. Cheng, A. de la Zerda, O. Gheysens, and S. S. Gambhir, "Noninvasive molecular imaging of small living subjects using Raman spectroscopy," *Proceedings of the National Academy of Sciences of the United States of America*, vol. 105, no. 15, pp. 5844–5849, 2008.

[5] Y. Dong and S.-S. Feng, "Poly(d,l-lactide-co-glycolide)/montmorillonite nanoparticles for oral delivery of anticancer drugs," *Biomaterials*, vol. 26, no. 30, pp. 6068–6076, 2005.

[6] C. Jin, L. Bai, H. Wu, W. Song, G. Guo, and K. Dou, "Cytotoxicity of paclitaxel incorporated in plga nanoparticles on hypoxic human tumor cells," *Pharmaceutical Research*, vol. 26, no. 7, pp. 1776–1784, 2009.

[7] S. Dhar, F. X. Gu, R. Langer, O. C. Farokhza, and S. J. Lippard, "Targeted delivery of cisplatin to prostate cancer cells by aptamer functionalized Pt(IV) prodrug-PLGA-PEG nanoparticles," *Proceedings of the National Academy of Sciences of the United States of America*, vol. 105, no. 45, pp. 17356–17361, 2008.

[8] Y. Inoue, K. Izawa, K. Yoshikawa, H. Yamada, A. Tojo, and K. Ohtomo, "In vivo fluorescence imaging of the reticuloendothelial system using quantum dots in combination with bioluminescent tumour monitoring," *European Journal of Nuclear Medicine and Molecular Imaging*, vol. 34, no. 12, pp. 2048–2056, 2007.

[9] X. Michalet, F. F. Pinaud, L. A. Bentolila et al., "Quantum dots for live cells, in vivo imaging, and diagnostics," *Science*, vol. 307, no. 5709, pp. 538–544, 2005.

[10] I. L. Medintz, H. T. Uyeda, E. R. Goldman, and H. Mattoussi, "Quantum dot bioconjugates for imaging, labelling and sensing," *Nature Materials*, vol. 4, no. 6, pp. 435–446, 2005.

[11] R. Weissleder, "A clearer vision for in vivo imaging," *Nature biotechnology*, vol. 19, no. 4, pp. 316–317, 2001.

[12] D. Shi, H. S. Cho, Y. Chen et al., "Fluorescent polystyrene-Fe_3O_4 composite nanospheres for in vivo imaging and hyperthermia," *Advanced Materials*, vol. 21, no. 21, pp. 2170–2173, 2009.

[13] Y. Inoue, K. Izawa, S. Kiryu, A. Tojo, and K. Ohtomo, "Diet and abdominal autofluorescence detected by in vivo fluorescence imaging of living mice," *Molecular Imaging*, vol. 7, no. 1, pp. 21–27, 2008.

[14] M. B. Bouchard, S. A. MacLaurin, P. J. Dwyer, J. Mansfield, R. Levenson, and T. Krucker, "Technical considerations in longitudinal multispectral small animal molecular imaging," *Journal of Biomedical Optics*, vol. 12, no. 5, Article ID 051601, 2007.

[15] J. R. Mansfield, K. W. Gossage, C. C. Hoyt, and R. M. Levenson, "Autofluorescence removal, multiplexing, and automated analysis methods for in-vivo fluorescence imaging," *Journal of Biomedical Optics*, vol. 10, no. 4, Article ID 41207, 9 pages, 2005.

[16] T. Troy, D. Jekic-McMullen, L. Sambucetti, and B. Rice, "Quantitative comparison of the sensitivity of detection of fluorescent and bioluminescent reporters in animal models," *Molecular Imaging*, vol. 3, no. 1, pp. 9–23, 2004.

[17] G. H. Krause and E. Weis, "Chlorophyll fluorescence as a tool in plant physiology," *Photosynthesis Research*, vol. 5, no. 2, pp. 139–157, 1984.

[18] R. Masuda, K. Kaneko, and I. Yamashita, "Sugar and cyclitol determination in vegetables by HPLC using postcolumn fluorescent derivatization," *Journal of Food Science*, vol. 61, no. 6, pp. 1186–1190, 1996.

[19] N. Ghosh, Y. Verma, S. K. Majumder, and P. K. Gupta, "A fluorescence spectroscopic study of honey and cane sugar syrup," *Food Science and Technology Research*, vol. 11, no. 1, pp. 59–62, 2005.

[20] G. Weagle, P. E. Paterson, J. Kennedy, and R. Pottier, "The nature of the chromophore responsible for naturally occurring fluorescence in mouse skin," *Journal of Photochemistry and Photobiology, B: Biology*, vol. 2, no. 3, pp. 313–320, 1988.

[21] G. A. Ritchie, "Chlorophyll fluorescence: what is it and what do the numbers mean?" in *National Proceedings: Forest and Conservation Nursery Associations—2005*, L. E. Riley, R. K. Dumroese, and T. D. Landis, Eds., Tech Coordinates, pp. 34–42, Department of Agriculture, Forest Service, Rocky Mountain Research Station, Fort Collins, Colo, USA, 2006.

[22] H. He, T. Zhu, R. Yu, Z. Gu, and H. Xu, "Study of fluorescence spectra of starch suspension excited by 260-nm UV light," *Chinese Optics Letters*, vol. 3, supplement 1, pp. 340–342, 2005.